THE HOST GALAXIES OF THREE RADIO-LOUD QUASARS: 3C 48, 3C 345, AND B2 1425+267[1]

SOFIA KIRHAKOS AND JOHN N. BAHCALL
Institute for Advanced Study, School of Natural Sciences, Princeton, NJ 08540

DONALD P. SCHNEIDER
Department of Astronomy and Astrophysics, Pennsylvania State University, University Park, PA 16802

AND

JEROME KRISTIAN[2]
Observatories of the Carnegie Institution of Washington, Pasadena, CA 91101

ABSTRACT

Observations with the Wide-Field/Planetary Camera-2 of the *Hubble Space Telescope* are presented for three radio-loud quasars: 3C 48 ($z = 0.367$), B2 1425+267 ($z = 0.366$), and 3C 345 ($z = 0.594$). All three quasars have luminous ($\sim 4 \times L^*$) galaxies as hosts, which are either elliptical (B2 1425+267 and 3C345) or interacting (3C 48), and all hosts are 0.5–1.0 mag bluer in $V - I$ than other galaxies with the same overall morphology at redshifts similar to those of the quasars. The host of 3C 48 has many H II regions and a very extended tidal tail. All nine of the radio-loud quasars studied here and in a previous paper by Bahcall et al. either have bright elliptical hosts or occur in interacting systems. There is a robust correlation between the radio emission of the quasar and the luminosity of host galaxy; the radio-loud quasars reside in galaxies that are on average ~ 1 mag brighter than hosts of the radio-quiet quasars.

Subject headings: galaxies: interactions — galaxies: structure — quasars: general — radio continuum: galaxies

1. INTRODUCTION

The characteristics of the host galaxies in which quasars reside may provide clues about the mechanisms that produce the observed energetic phenomena. To understand quasars, we would like to know answers to the following key questions: What kind of galaxies display the quasar phenomena? How old are the galaxies? Do the hosts show signs of interactions or of star formation? How are the quasars fed? How long is a quasar active in any galaxy? What fraction of galaxies show quasar phenomena?

The search for quasar host galaxies to help answer these questions was initiated by the pioneering work, using photographic plates, of Kristian (1973) and Wyckoff et al. (1980). The use of two-dimensional electronic detectors and CCDs made possible major improvements in the studies of quasar environments; some representative papers are Hutchings, Janson, & Neff (1989), Hutchings & Neff (1992), Dunlop et al. (1993), and McLeod & Rieke (1994a, 1994b). These ground-based studies indicated the presence of host galaxies of many quasars and suggested that some of the hosts appeared to be disturbed by a gravitational encounter (e.g., Hutchings & Campbell 1983; Hutchings, Crampton, & Campbell 1984). Several spectroscopic studies of the nebulosity surrounding quasars have indicated that the nature of the emission is starlight from the underlying galaxy (Boroson, Oke, & Green 1982; Boroson & Oke 1982, 1984; Balick & Heckman 1983; Kukula et al. 1996). In particular, Kukula et al. obtained optical off-nuclear spectra of active galaxies and estimated the ages of the stellar populations using spectral synthesis models.

The *Hubble Space Telescope HST* opened a new window to the study of quasar host galaxies. The high angular resolution of the *HST* has produced spectacular images of a number of quasars (Bahcall et al. 1994, 1995a, 1995b, 1996a, 1996b, 1997; Hutchings et al. 1994; Disney et al. 1995; Hutchings & Morris 1995; Boyce et al. 1996; Hooper et al. 1997). The *HST* images also revealed the presence of surprisingly close companions; for example, PKS 2349+014 (Bahcall et al. 1995a) has a companion galaxy located only 3.5 kpc in projection (for $H_0 = 100$ km s^{-1} Mpc^{-1} and $\Omega_0 = 1.0$) from the quasar center.

In Bahcall et al. (1996b, 1997), we reported the results of our study of 20 nearby ($z < 0.30$) luminous quasars observed with the *HST* Wide-Field/Planetary Camera-2 (WFPC2) in F606W. The quasars in this local sample occur in diverse environments that include bright ellipticals, apparently normal elliptical and spiral galaxies, very faint hosts, and complex systems of gravitationally interacting components. The hosts of all six radio-loud quasars (RLQs) in the sample are bright elliptical galaxies or interacting systems. However, contrary to widespread expectations based on ground-based observations of radio galaxies and Seyfert galaxies (see Balick & Heckman 1982 and references therein), the radio-quiet quasars (RQQs) occur in both elliptical *and* spiral galaxies. A tendency for high-luminosity quasars to occur in early type galaxies was suggested by McLeod & Rieke (1995b). A similar result was obtained by Taylor et al. (1996) based on ground-based near-infrared imaging. Only six RLQs are included in the local sample, which motivates us to obtain observations of more RLQs to better understand the connection between the radio emission and the quasar environment.

In this paper, we present *HST* WFPC2 observations of three additional RLQs: 3C 48, B2 1425+267, and 3C 345. Their redshifts are 0.367, 0.366, and 0.594, respectively, higher than all the redshifts of the local sample quasars and

---

[2] Deceased.

F555W   F814W

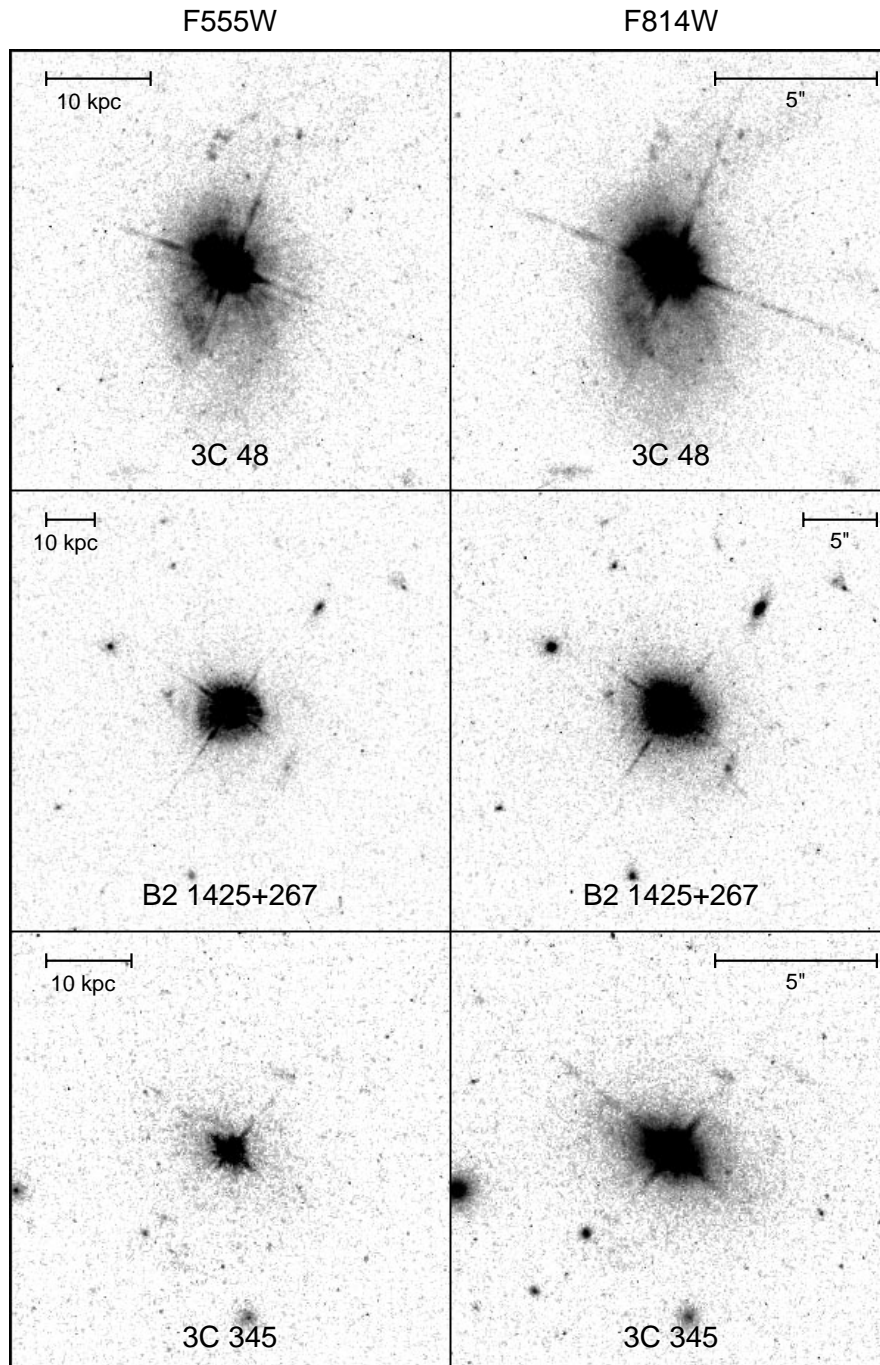FIG. 1.—Figure shows the 14″ × 14″ PC images of 3C 48 and 3C 345 and 30″ × 30″ WF3 images of B2 1425+267 taken with filters F555W (*left-hand panels*) and F814W (*right-hand panels*). The images shown are the average of two 1400 s exposures in F555W and two 1700 s exposures in F814W (see Table 1). Cosmic-ray subtraction and pipeline STScI flat-fielding are the only processing performed on the data. The images have been rotated in order to have north on top and east to the left.

comparable to the objects studied by Hooper et al. (1997). The optical luminosities of the three quasars are in the range of luminosities covered by our local sample but are on average significantly more luminous than those of the Hooper et al. (1997) sample. 3C 48 is a compact steep spectrum radio source, with strong asymmetric emission with respect to the core and a subarcsecond radio jet (Fanti et al. 1995; Simon et al. 1990). B2 1425+267 is a double-lobed radio source, with angular size of 240″ (Rogola, Padrielli, &

de Ruiter 1986). 3C 345 is a superluminal source, with an unresolved flat radio spectrum and a radio jet extending out to several arcseconds (Kollgaard, Wardle, & Roberts 1989).

This paper is organized as follows. In § 2 we describe the observations; in § 3 we describe the subtraction of the point-spread function (PSF) and the methods of analyzing of the data; in § 4 we report on the magnitudes and colors measured for the host galaxies; in §§ 5–7 we discuss individually the hosts of 3C 48, B2 1425+267, and 3C 345, respec-

TABLE 1

JOURNAL OF OBSERVATIONS

Quasar	Date	Filter	CCD	Sky Level $(e^{-}\ \mathrm{pixel}^{-1}\ \mathrm{s}^{-1})$	z[a]	V_{QSO}[a]	Kiloparsec[b] (arcsec^{-1})	$M_{V(QSO)}$[b, c]
3C 48	1995 Jan 21	F555W	PC1	0.015	0.367	16.20	3.08 (6.62)	−24.0 (−25.7)
	1995 Jan 21	F814W	PC1	0.014				
	1996 Jan 30	FR680N18[d]	WF2	<0.001				
B2 1425+267	1994 Dec 02	F555W	WF3	0.085	0.366	15.68	3.07 (6.61)	−24.5 (−26.2)
	1994 Dec 02	F814W	WF3	0.085				
3C 345	1994 Oct 20	F555W	PC1	0.009	0.594	15.96	3.79 (8.51)	−25.3 (−27.0)
	1994 Oct 20	F814W	PC1	0.008				

[a] From Véron-Cetty & Véron 1996.
[b] Computed for $\Omega_0 = 1.0$ and $H_0 = 100\ \mathrm{km\ s}^{-1}\ \mathrm{Mpc}^{-1}$ ($\Omega_0 = 0.2$ and $H_0 = 50\ \mathrm{km\ s}^{-1}\ \mathrm{Mpc}^{-1}$).
[c] We assumed that the spectrum of quasars can be described by a power law of the form $f_v \propto v^{-0.5}$.
[d] Linear ramp filter centered at 6845 Å, which covers the [O III] $\lambda5007$ emission at the quasar redshift.

tively; in § 8 we discuss the presence of companion galaxies; and in § 9 we summarize and discuss our results. Through this paper we assume that $H_0 = 100\ \mathrm{km\ s}^{-1}\ \mathrm{Mpc}^{-1}$ and $\Omega_0 = 1.0$ unless we note otherwise. When we quote distances and luminosities from papers that used different cosmological parameters, we have transformed the values to the $H_0 = 100\ \mathrm{km\ s}^{-1}\ \mathrm{Mpc}^{-1}$ and $\Omega_0 = 1.0$ system.

2. OBSERVATIONS

The quasars 3C 48, B2 1425+267, and 3C 345 were observed with the WFPC2 (see Biretta et al. 1996) through the F555W and F814W filters, which correspond approximately to the V and I bandpasses, respectively. Redshifted [O II] $\lambda3727$ and [O III] $\lambda4363$ are included in the F555W bandpass of the three quasars; for 3C 345, redshifted Hβ and [O III] $\lambda\lambda4959, 5007$ are also included in the F814W band. B2 1425+267 was placed near the center of the Wide-Field Camera CCD 3 (WF3), while 3C 48 and 3C 345 were placed near the center of the Planetary Camera (PC). Four images of each quasar were obtained in each filter: two short exposures (50 s) to investigate the small-scale structure close to the nucleus, and two long exposures (1400 s in F555W and 1700 s in F814W) to examine the parent galaxy, nearby galaxies, and other extended structure.

The image scales of the PC and WF3 are 0″0455 pixel^{-1} and 0″0996 pixel^{-1}, respectively. The adopted photometric zero point for 1 $e\ \mathrm{s}^{-1}$ is 24.58 mag for the F555W filter and 24.13 mag for the F814W band (Biretta et al. 1996).

Narrowband images, centered at redshifted [O III] $\lambda5007$ emission, were obtained of 3C 48 using the linear ramp filter FR680N18. The FR680N18 filter covers the wave band from 6800 to 6921 Å (rest wavelengths of 4974–5063 Å). The linear ramp filters are divided into four parallel strips where the central wavelength across each strip varies by $\sim 6\%$. Each CCD pixel is mapped to a unique central wavelength with a FWHM bandwidth of approximately 1.3% of the central wavelength (Biretta et al. 1996). Three exposures of 1100, 1300, and 1100 s were obtained.

The initial data processing (bias frame removal and flat-field calibration) of the broadband images was performed at the Space Telescope Science Institute with their standard software package. The narrowband images were not flat-fielded in the STScI calibration pipeline; we obtained the appropriate flat-field reference image from the *HST* archive and flattened the data. Cosmic rays were identified by a pixel-by-pixel comparison of pairs of images of similar exposure time; the intensity of a pixel containing a cosmic

ray was replaced by the scaled value of the intensity of the pixel in the other image. The calibration of the [O III] image was done using the Linear Ramp Filter Calculator and following standard procedures described in the STScI-WFPC2 World Wide Web home page.

Figure 1 shows the three RLQs in the F555W and F814W bands. The host galaxies of 3C 48 and 3C 345 are clearly visible in the F814W images; the host of B2 1425+267 is less prominent but can be seen with confidence upon careful inspection of the F814W image. A journal of the observations is given in Table 1.

3. DATA ANALYSIS

The most challenging aspect of the data analysis is removal of the signal due to the quasar nucleus, which is a heavily saturated point source in the long exposures. We performed PSF subtraction and subsequent analysis using the techniques described in Bahcall et al. (1997). Briefly, we found a best-fit subtraction for each image by performing a χ^2 minimization of the residuals in an annulus between 1″ and 3″ away from the quasar center. We used empirical (WFPC2 images of stars) and model PSFs constructed using the Tiny Tim software (Krist 1993), which resulted in host galaxy magnitudes that agreed within 0.2 ± 0.1 mag. Subsequently, all analysis was performed using the Tiny Tim–subtracted images. Figure 2 shows the three quasars after subtraction; galaxy parameters derived from these images are given in Table 2.

We determined host galaxy magnitudes by analyzing the PSF-subtracted images using the three techniques detailed in Bahcall et al. (1997): aperture photometry outside of the nucleus is shown in Table 3, and one-dimensional fits of disk and de Vaucouleurs (1948) profiles to azimuthally averaged radial profiles and two-dimensional fits of disk and de Vaucouleurs laws to the images themselves are shown in Table 4. The parameters and results of these analyses are given in Tables 3 and 4. The one- and two-dimensional fits are in excellent agreement. Both approaches yield somewhat brighter magnitudes than the aperture photometry, as expected because the annular apertures omit light from the bright central parts of the hosts.

To check for a possible effect of the PSF subtraction on the color of the host galaxies we also performed two-dimensional fits on the unsubtracted quasar images: the amplitude of the point source was fitted simultaneously with the galaxy. The root mean square (rms) difference between the host galaxies magnitudes obtained with the
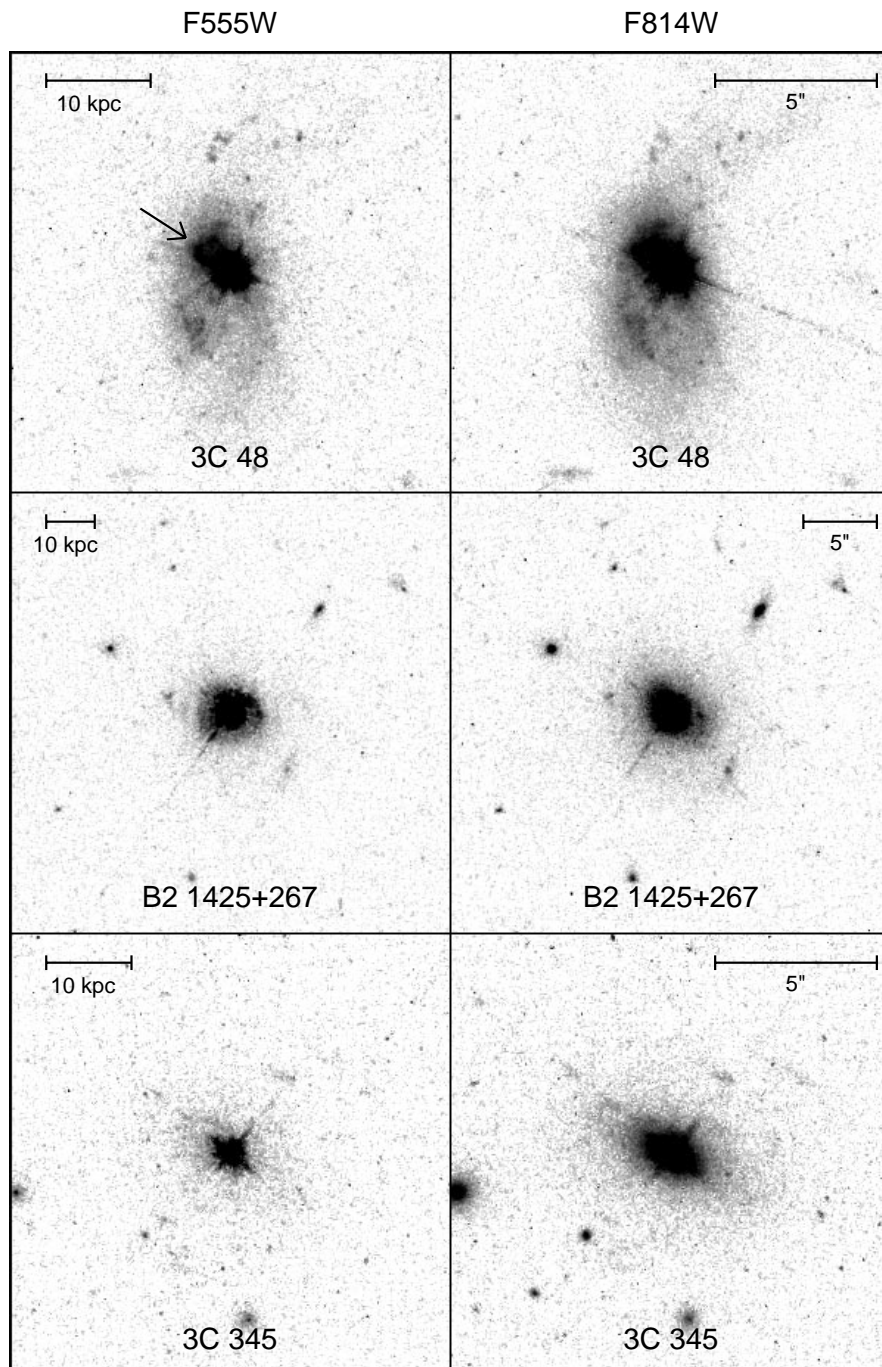
F555W F814W

FIG. 2.—Same display as shown in Figure 1, but with a best-fit PSF subtracted from the data. An arrow in the F555W image of 3C 48 indicates a ring feature that may be an optical artifact.

two-dimensional fits to the unsubtracted and to the PSF-subtracted quasar images is less than 0.3 mag; the rms difference in color, $m_{F555W} - m_{F814W}$, is 0.1 mag.

4. MAGNITUDES AND COLORS OF HOST GALAXIES

Figure 3 compares the measured colors, $m_{F555W} - m_{F814W}$, for the three hosts with the predicted galaxy colors for different morphological types. For the normal galaxy colors, we use the results of Fukugita, Shimasaku, & Ichikawa (1995). All the three host galaxies have $m_{F555W} - m_{F814W}$ colors at least 1 mag bluer than predicted for elliptical hosts at the same redshift.

Do the bluer colors indicate that the light from the quasar is contaminating the measurements? To investigate this possibility, we measured the $m_{F555W} - m_{F814W}$ color in a large annular aperture centered on the quasar. The large-aperture colors average only 0.13 mag redder than the two-dimensional fit; $m_{F555W} - m_{F814W} = +0.7, +1.0,$ and $+1.3$ for 3C 48, B2 1425+267, and 3C 345, respectively, for annular aperture radii $1\rlap{.}''4$–$5\rlap{.}''5$, $3\rlap{.}''0$–$4\rlap{.}''0$, and $1\rlap{.}''4$–$2\rlap{.}''3$. We conclude that the bluer colors of the host galaxies are not the result of contamination by quasar light. In plotting the colors of the host galaxies shown in Figure 3, we used the average of the large annular aperture and the two-

TABLE 2
SIZE AND MORPHOLOGY OF HOST GALAXIES

		MAJOR DIAMETER			
QUASAR	FILTER	(arcsec)	(kpc)[a]	ISOPHOTE (mag arcsec^{-2})	MORPHOLOGY (apparent)
3C 48	F555W	8.5	26 (56)	23.3	Interacting
3C 48	F814W	9.8	30 (65)	23.2	Interacting
B2 1425+267......	F555W	11.2	34 (74)	25.2	E1
B2 1425+267......	F814W	14.2	44 (94)	25.1	E3
3C 345	F555W	4.5	17 38)	23.8	E2
3C 345	F814W	6.5	25 (55)	23.6	E3

[a] Computed for $\Omega_0 = 1.0$ and $H_0 = 100$ km s^{-1} Mpc^{-1} ($\Omega_0 = 0.2$ and $H_0 = 50$ km s^{-1} Mpc^{-1}).

dimensional fit photometry as the "best estimate" and one-half the difference between the two methods as a measure of the uncertainty.

The measured colors suggest that the host galaxies of the three RLQs contain a younger stellar population than expected for elliptical or spiral galaxies at the redshifts of the quasars.

The estimated absolute V and I magnitudes of the quasar hosts are included in Tables 3 and 4; the measured F555W and F814W magnitudes were transformed to V and I by applying k-corrections calculated by Fukugita et al. (1995). Figure 3 shows that the $m_{F555W} - m_{F814W}$ color indices for the hosts of 3C 48 and B2 1425+267 are close to the predicted values for irregular galaxies at redshifts similar to those of the quasars, while for the host of 3C 345, the measured color index is between that predicted for irregulars and Scd galaxies. Given the redshift of the quasars and the morphological type inferred from Figure 3, we used Tables 6–8 from Fukugita et al. (1995) to obtain the m_{F555W}

$- V$ and $m_{F814W} - I$ colors, and we used their Figure 10 to obtain the k-correction in V and I.

5. 3C 48 (0134+32)

The radio loud source 3C 48 was the first quasar to be identified optically (Matthews et al. 1961). The first deep images of 3C 48 revealed extended emission and suggested that quasars were associated with the centers of galaxies. 3C 48 was also the first quasar to be shown to have a spatially resolved emission-line region (Wampler et al. 1975).

5.1. Broadband and [O III] Images

The WFPC2 broadband images, Figures 1, 2, and 4, show that 3C 48 is surrounded by extensive nebulosity, is permeated with brighter spots (probably H II regions), and has traces of faint tidal tails that extend tens of kiloparsecs. The morphology of the host of 3C 48 indicates that strong gravitational interaction has taken place, which confirms the evidence of merging suggested by previous studies (see

TABLE 3
MAGNITUDES OF THE QUASAR HOST GALAXIES: APERTURE PHOTOMETRY

Quasar	Inner radius (arcsec)	Outer Radius (arcsec)	m_{F555W}	$m_{F555W} - m_{F814W}$	M_V[a]	M_I[a]
3C 48	0.3	5.5	18.1	+0.7	−22.3 (−23.9)	−23.2 (−24.8)
B2 1425+267......	0.6	4.0	19.1	+0.7	−21.3 (−22.9)	−22.2 (−23.8)
3C 345	0.3	2.3	20.0	+1.3	−21.0 (−22.8)	−22.8 (−24.6)

[a] Computed for $\Omega_0 = 1.0$ and $H_0 = 100$ km s^{-1} Mpc^{-1} ($\Omega_0 = 0.2$ and $H_0 = 50$ km s^{-1} Mpc^{-1}); k-corrections are from Fukugita et al. 1995.

TABLE 4
MAGNITUDES OF THE QUASAR HOST GALAXIES: ANALYTIC GALAXY MODEL FITS

Quasar	m_{F555W}	r[a] (arcsec)	m_{F814W}	r[a] (arcsec)	$m_{F555W} - m_{F814W}$	Best Model	M_V[b]	M_I[b]
					One-Dimensional			
3C 48	17.9	1.2	17.1	0.9	+0.8	GdV	−22.5 (−24.1)	−23.5 (−25.1)
B2 1425+267......	18.4	1.5	17.8	1.5	+0.6	GdV	−22.0 (−23.6)	−22.8 (−24.4)
3C 345	19.4	0.3	18.1	0.8	+1.3	GdV	−21.6 (−23.4)	−23.4 (−25.2)
					Two-Dimensional			
3C 48	17.7	2.5	17.2	1.8	+0.5	GdV	−22.7 (−24.3)	−23.4 (−25.0)
B2 1425+267......	18.3	2.0	17.6	2.7	+0.7	GdV	−22.1 (−23.7)	−23.0 (−24.6)
3C 345	19.6	0.5	18.2	0.6	+1.4	GdV	−21.4 (−23.2)	−23.3 (−25.1)

[a] Effective radius.
[b] Computed for $\Omega_0 = 1.0$ and $H_0 = 100$ km s^{-1} Mpc^{-1} ($\Omega_0 = 0.2$ and $H_0 = 50$ km s^{-1} Mpc^{-1}); k-corrections are from Fukugita et al. 1995.
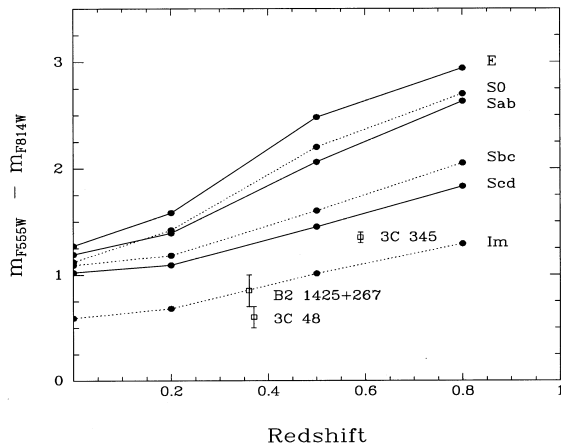
FIG. 3.—Predicted $m_{F555W} - m_{F814W}$ color indices for different galaxy morphological types as a function of the redshift, from Fukugita et al. (1995). The color indices for the three quasar host galaxies (from two-dimensional fits listed in Table 4) are indicated.

Stockton & Ridgway 1991 and references therein). The F555W and F814W images look similar to one another, although the tidal tails and extended nebulosity are more prominent in the F814W image. The F814W image of 3C 48 was published by Canalizo, Stockton, & Roth (1998) when

they reported the discovery of a broad absorption-line quasar at $z = 2.169$ located 41″ southwest of 3C 48.

The tidal tail extends for ~ 35 kpc at P.A. $\sim 330°$ (we adopt the standard convention for position angle: north is at P.A. $= 0°$ and east at P.A. $= 90°$); it then curves almost in a right angle to the southwest for another ~ 20 kpc. The surface brightness of the tidal tail in the F814W images ranges from 23.2 mag arcsec^2 at $\sim 4″$ (12 kpc) from the quasar center to ~ 25 mag arcsec^2 at the outer parts. The faint-nebulosity tail can be seen in the F814W image in Figure 4 (upper right-hand portion).

The WFPC2 broadband images reveal a bright region centered at $\sim 1″.2$ northeast from the center of the quasar (see Fig. 2). The morphology of this feature is complex; on top of the higher surface brightness region there is a ring (indicated by an arrow in the F555W image in Fig. 2). This ring feature resembles ghost images seen in previous WFPC2 data (PG 1307+085; Bahcall et al. 1997), so the ring may be an optical artifact. The morphology of the northeast bright emission region is similar in both F555W and F814W images.

Figure 4 compares the broadband and the [O III] $\lambda 5007$ images of 3C 48, in which the brightest knots are marked with roman letters for identification. These knots are listed in Table 5. The upper panels show the F555W (left) and F814W (right) images with a linear scale that matches that
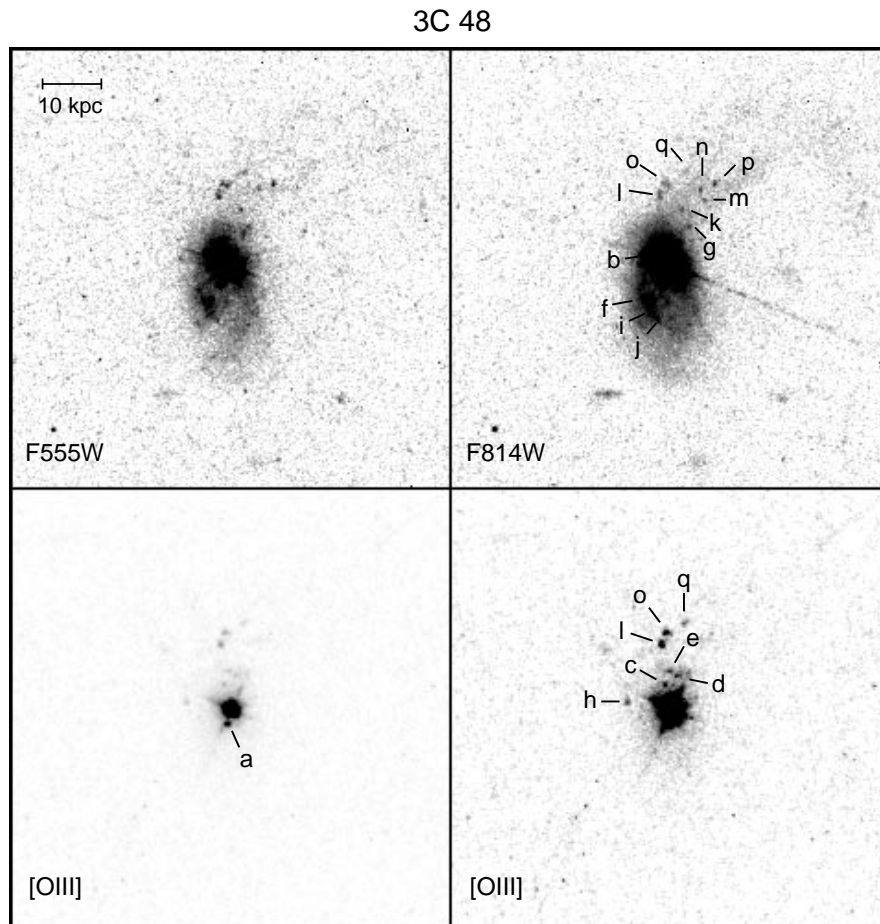
3C 48

FIG. 4.—Bright knots observed in the broadband and [O III] $\lambda 5007$ images of the 3C 48 host galaxy. The upper panels show the F555W (left) and F814W (right) images. The lower panels show the [O III] image taken with the linear ramp filter FR680N18. The lower left-hand panel has a higher contrast stretch to show the bright [O III] knot at 0″.8 to the south of the quasar. The knots are identified by roman letters and listed in Table 5. Each image is 24″ on a side with north at the top and east to the left. The [O III] image was taken with the WF2 while the F555W and F814W images were taken with the PC.

TABLE 5

BRIGHT KNOTS OBSERVED IN THE BROADBAND AND [O III] IMAGES OF THE HOST GALAXY OF 3C 48

d (arcsec)	$\Delta\alpha$ (arcsec)	$\Delta\delta$ (arcsec)	Aperture[a] Radius (arcsec)	m_{F814W} (mag)	m_{F555W} (mag)	[O III] flux[b] (10^{-16} ergs cm^{-2} s^{-1})	Region[c]
0.8......	0.2	−0.8	...	...	...	23.6	a
1.1......	1.0	0.5	0.2	21.8	22.6	...	b[d]
1.4......	0.3	1.4	0.3	22.8	24.0	2.9	c
1.8......	−0.2	1.8	...	...	...	2.3	d
2.1......	0.1	2.1	...	...	...	2.2	e
2.1......	1.2	−1.7	0.4	23.5	...	...	f
2.2......	−0.8	2.0	0.2	25.6	23.5	...	g
2.4......	0.9	−2.2	0.1	24.8	25.1	...	h
2.5......	2.5	0.4	...	...	26.2	2.9	i
2.7......	0.6	−2.6	0.1	25.1	26.7	...	j
2.8......	−0.5	2.8	0.2	25.9	25.5	...	k
3.6......	0.6	3.6	0.3	24.4	24.6	8.1	l
3.7......	−1.6	3.3	0.1	25.6	...	...	m
4.1......	−1.4	3.8	0.2	25.4	25.9	...	n
4.1......	0.3	4.1	0.3	24.6	24.5	7.1	o
4.6......	−2.1	4.1	0.2	24.7	25.0	...	p
4.7......	−0.6	4.7	0.3	25.4	25.7	2.8	q

[a] Broadband images.
[b] Measured within a 0″.3 radius.
[c] Nomenclature from Fig. 4.
[d] This knot is probably part of an image artifact (see § 5.1).

of the [O III] image (*lower panels*). The lower right-hand panel of Figure 4 shows the [O III] image with a high-contrast stretch to maximize the visibility of the bright H II region at 0″.8 south of the quasar. We do not detect a counterpart for this emitting region in the F555W and F814W images. There are five knots in common between the [O III] and the broadband images: c, i, l, o, q.

5.2. Comparison with Previous Studies

Boroson & Oke (1982) obtained spectra of the faint nebulosity 2″ north and south of the center of 3C 48. They detected narrow emission lines ([O II] $\lambda3727$, [O III] $\lambda\lambda4959$, 5007, and [O I] $\lambda6300$) plus a continuum dominated by hot stars at both positions, which suggests that the host is a spiral galaxy. Stellar absorption lines were also detected in the nebulosity; the integrated light has both a $B-V$ color and absorption features indicative of middle-to-late A stars, which suggests that a massive star formation burst was triggered $\sim10^8$ yr ago. Boroson & Oke (1982) estimated that the magnitude of the host at 5500 Å is ~18.5 mag. This is in qualitative agreement with the magnitude we estimated with the one-dimensional model fit (17.9 mag).

Malkan (1984) reports a blue $v-g$ color for the 3C 48 host, consistent with Boroson and Oke's spectroscopy. Malkan suggests that the host of 3C 48 is an elliptical galaxy that has brightened as a result of a burst of star formation; fitting a de Vaucouleurs (GdV) model to the luminosity profile, Malkan estimates the host galaxy to have $M_B = -22.4$ and $r_{\rm eff} = 16$ kpc. Applying the Fukugita et al. (1995) color transformation relations, the host galaxy measured by Malkan is ~0.7 mag brighter in V than our measurements, and the effective radius quoted by Malkan is a factor ~2 larger than the value given by our two-dimensional model (see Table 4).

Stockton & Ridgway (1991) obtained a narrowband image of 3C 48 centered on the [O III] $\lambda5007$ line and three line-free band images centered at 0.58, 0.77, and 2.1 μm. In the continuum images, Stockton & Ridgway detected a

high surface brightness region centered at ~1 ″ to the northeast of the quasar nucleus, which they suggested might be the nucleus of a galaxy in the process of merging with the host galaxy of 3C 48 (they designated this region 3C 48A). We detected a bright emission region at approximately the same position as 3C 48A in the F555W and F814W images. In our broadband *HST* images, the morphology of this feature is complex and might be contaminated by a ghost image (see the arrow in Fig. 2). We do not detect an obvious secondary nucleus in this region.

In their [O III] image, Stockton & Ridgway (1991) detected diffuse emission surrounding the quasar, and some bright knots, mostly to the north and west. The brightest [O III] emitting region is $\sim3″.8$ north to the nucleus, corresponding to the bright knots l and o in our Figure 4. Stockton & Ridgway pointed out that the presence of this bright [O III] emission region to the north of the quasar explained why many authors found a strong asymmetry in the detection of emission in spectroscopic observations centered $\sim4″$ north and south of the quasar.

The radio structure of 3C 48 at 329 MHz shows a one-sided convoluted jet extending for $\sim0″.5$ to the north of the quasar and fainter emission extending to the east (Simon et al. 1990). Akujor et al. (1994) obtained a MERLIN image of 3C 48 at 18 cm, which slightly resolves the structure of the compact radio source. The radio emission extends slightly along the north-south direction, as does the host galaxy nebulosity seen in the F555W and F814W images. We have searched for the optical counterpart of the radio jet in our *HST* images but failed to detect one; we set an upper limit of 22.2 mag arcsec^{-2} in the F814W band.

6. B2 1425+267 (TON 202)

In the F814W band image, the host of B2 1425+267 appears to be an elliptical galaxy, while in the F555W image, the host galaxy appears rounder and displays an arclike feature at an average distance from the quasar of 1″.5. We have inspected dozens of WFPC2 images of stars in

our search for a stellar PSF to match the present quasar images; none of the stellar images possess a feature like the arc seen in B2 1425+267. The arc could, in principle, be a spiral arm or the debris trail of a small galaxy disrupted by the quasar host; better images are required to reach a definitive conclusion. The results of the one- and two-dimensional fits are consistent with the host of B2 1425+267 being an elliptical galaxy. In the absence of definitive evidence to the contrary, we adopt the E-galaxy classification as being the simplest interpretation of the available images.

There are a number of suggestions in the literature that B2 1425+267 is an interacting system. For example, Stockton & MacKenty (1983) suggested that the morphology of the extended emission-line regions around B2 1425+267 resulted from interactions between two galaxies of similar masses. Also, Hutchings et al. (1984) obtained ground-based B band images of B2 1425+267 and described the host galaxy as irregular and possibly interacting with a companion. There are some signs in the WFPC2 images that interaction might be present; however, it is clear that any interaction that is occurring does not involve a galaxy of luminosity and size comparable to that of the host galaxy.

We detect two faint resolved sources within the host galaxy, which coincide approximately with the extended emission-line gas detected by Stockton & MacKenty (1983, 1987). One source is at $\sim 1\rlap{.}''9$ (5.8 kpc, P.A. = 264°) from the center of the quasar, with $m_{F814W} = 24.0$ mag. This feature is more prominent in the F814W image but also appears as a higher surface brightness spot in the F555W image, on top of the arclike feature. The second source has $m_{F814W} = 24.2$ mag and is located $4\rlap{.}''3$ (13.2 kpc, P.A. = 75°) from the quasar.

A large number of galaxies surround B2 1425+267 in the WFPC2 images; three are within 10″ (30 kpc) of the center of the host galaxy. Block & Stockton (1991) detected these galaxies in their ground-based R-band image and called them A, B, and C. In the HST images galaxy A is at $9\rlap{.}''2$ (P.A. = 62°), galaxy B at $9\rlap{.}''1$ (P.A. = 319°), and galaxy C at $5\rlap{.}''4$ (P.A. = 223°); their magnitudes in the F814W image are 21.9, 21.7, and 23.1 mag, and their colors $m_{F555W} - m_{F814W}$ are +1.2, +1.4, and +0.8 mag, respectively. Galaxy C and the quasar host galaxy have similar colors, while galaxies A and B are redder. Galaxy C lies within the nebulosity of the quasar host galaxy; there is no indication that the host galaxy extends to galaxies A and B.

Spectroscopic observations at 3″ from the nucleus by Boroson, Person, & Oke (1985) revealed several emission lines in the nebulosity, including Hα, Hβ and [O III], and some continuum emission as well. Malkan (1984) detected a bright host for B2 1425+267, probably an elliptical galaxy, with $M_B = -22.1$ and $r_{eff} = 17$ kpc. Applying the Fukugita et al. (1995) color transformation relations, the host galaxy measured by Malkan is $\gtrsim 1$ mag brighter in V than our measurements, and the effective radius quoted by Malkan is a factor ~ 2 larger than the value given by our two-dimensional model (see Table 4).

7. 3C 345 (1641+399)

The bright radio source 3C 345 was optically identified by Goldsmith & Kinman (1965) shortly after the first quasars were discovered, and it soon became famous for its extreme variability in almost all wave bands. In the optical domain, 3C 345 is classified as a blazar, a subset of the

radio-loud active galactic nuclei (AGNs) for which the relativistic radio jet happens to point at small angles to the line of sight (Angel & Stockman 1980). The radio source 3C 345 exhibits apparent superluminal motion (Schraml et al. 1981) and high levels of optical and radio polarization. A one-sided radio jet extending for several arcseconds and a faint steep-spectrum giant halo are also present (Kollgaard, Wardle, & Roberts 1989).

The HST images reveal that the host galaxy of 3C 345 is a bright elliptical (E3) that is clearly seen in the F814W band. No prominent peculiar morphological features are present in the two HST images. Many galaxies are detected in the quasar field, including a bright elliptical, with $m_{F814W} = 20.7$, at 26 kpc projected separation ($\Delta\alpha = 6\rlap{.}''8$ and $\Delta\delta = -1\rlap{.}''3$) from the quasar. The measured redshift of this companion galaxy, $z = 0.5880$ (Ellingson & Yee 1994), is close to the quasar redshift ($z = 0.594$).

The position angle of the major axis of the host galaxy is $\sim 60°$ in the F814W image. The radio jet at several arcseconds from the core has P.A. = 330° (Kollgaard et al. 1989), approximately perpendicular to the main plane of the host galaxy. We do not detect an optical counterpart to the radio jet, but we cannot set strong limits to the optical emission as one of the diffraction spike remnants at P.A. = 320° extends for $1\rlap{.}''5$ from the quasar. The available observations show that the jet is fainter than 21.8 mag arcsec^{-2} in F814W.

8. COMPANION GALAXIES

We have systematically examined the HST images of the quasar fields for companion galaxies projected close to the quasars. To evaluate the statistical significance of the small projected separations of the quasar-galaxy pairs, we constructed a sample of "companion" galaxies using two criteria: a maximum projected metric displacement from the quasar and a minimum galaxy luminosity.

Table 6 lists all the galaxies that have $d_{proj} \leq 25$ kpc and $M_{F606W} \leq -16.5$; these are the values used for the local sample (Bahcall et al. 1997). The table contains the following information: the radius (arcseconds) used for the photometric measurement, the projected distance from the quasar (in arcseconds and kiloparsec), the apparent magnitude in the F814W band, the color index ($m_{F555W} - m_{F814W}$), and the estimated apparent and absolute magnitudes in F606W. To determine the brightness of the companion galaxies in the F606W band, we first verified, using Figure 3, which morphological type corresponded to the measured color $m_{F555W} - m_{F814W}$. The color transformation tables of Fukugita et al. (1995) were used to obtain $m_{F606} - m_{F555W}$ for each companion galaxy.

As described in § 6 of Bahcall et al. 1995b, to evaluate the statistical significance of the close companions observed, we built a comparison sample by counting galaxies in similar regions imaged at the same time and with the same instrumental configuration as each of the quasar fields. We counted galaxies in circular areas that are within 25 kpc (at the quasar redshift) of the quasar position shifted to CCD 2 and CCD 4; the quasar images in the local sample are all close to the center of CCD 3 of the WFC2.

In the 40 fields of CCD 2 and CCD 4 that accompany the 20 quasar images of the local sample, there are eight galaxy companions that would have satisfied the a priori criteria for inclusion in our complete sample of close companions had they been found at the same coordinate positions in CCD 3. For three fields, the expected number of compan-

TABLE 6

GALAXY COMPANIONS WITH M_{F606W} BRIGHTER THAN -16.5 MAG WITHIN 25 KPC (~ 55 KPC)[a] OF THE QUASAR

			DISTANCES					
QUASAR	NUMBER OF COMPANIONS	APERTURE RADIUS (arcsec)	(arcsec)	(kpc)[a]	m_{F814W}	$m_{F555W} - m_{F814W}$	m_{F606W}[b]	M_{F606W}
3C 48	1	0.7	7.0	21.5 (46.3)	23.4	+0.9	23.9	−16.5
B2 1425+267	1	1.0	5.4	16.6 (35.7)	23.1	+0.8	23.4	−17.0
3C 345	3	0.3	2.8	10.6 (23.8)	23.9	+1.1	24.6	−16.9
		0.2	3.6	13.7 (30.6)	23.3	+2.0	24.7	−16.8
		0.4	5.1	19.3 (43.4)	23.0	+0.6	23.3	−18.2

[a] Computed for $\Omega_0 = 1.0$ and $H_0 = 100$ km s^{-1} Mpc^{-1} ($\Omega_0 = 0.2$ and $H_0 = 50$ km s^{-1} Mpc^{-1}).
[b] Color transformation from Fukugita et al. (1995). See § 8 for details.

ions would be 0.60. The Poisson probability of finding five or more projected close galaxy companions as listed in Table 6 is

$$P(\geq 5, 0.6; 25 \text{ kpc}, M_{F606W} \leq -16.5) \leq 0.0004 . \quad (1)$$

If we use the eight WF frames that accompany the three RLQs to draw a control sample, we find six galaxies that satisfy the selection criteria. For three fields, the expected number of companions would be 2.3. The Poisson probability of finding five or more projected close galaxy companions is

$$P(\geq 5, 2.3; 25 \text{ kpc}, M_{F606W} \leq -16.5) \leq 0.05 . \quad (2)$$

We conclude that the presence of the projected close companions around the three RLQs is statistically significant. A similar result was found by Bahcall (1995b, 1997) and Fisher et al. (1996) for the local sample.

Ellingson & Yee (1994) measured the redshifts of 31 galaxies in the field of 3C 345. Eight of their galaxies have velocities within 3000 km s^{-1} of the quasar. Five of those galaxies are included in the *HST* images, although only one of them is close enough to appear in the field of view shown in Figures 1 and 2.

The five galaxies in the *HST* images known to be at the same distance as 3C 345 have measured colors $m_{F555W} - m_{F814W}$ that are consistent to the colors expected for normal galaxies of similar morphology and redshift.

9. DISCUSSION

The main results of this study are the following: (1) the three RLQs studied have bright (several L^*) host galaxies; (2) the hosts of RLQs are, on average, about 1 mag more luminous than the hosts of RQQs; and (3) the host colors $m_{F555W} - m_{F814W}$ are substantially bluer than expected for galaxies of similar morphological types at the same redshifts as the quasars.

9.1. *Nature of the Hosts*

Ground-based observations have produced contradictory evidence regarding the stellar populations of the quasar hosts galaxies. Orndhal, Ronnback, & van Groningen (1996) report that quasar host galaxies have $V - R$ colors typical of late-type spirals, whereas Kukula et al. (1996) concluded from near-infrared observations that the noninteracting hosts of RLQs are systems with old, red stellar populations. The ability of *HST* to address this question suggests that one should further investigate the colors

of the hosts of the low-redshift quasars to determine whether (1) the host galaxies of luminous quasars are generally bluer than "normal" galaxies of similar morphological type, (2) host galaxies of RLQs are bluer than the hosts of RQQs, or (3) we are witnessing an extraordinary evolutionary effect in the colors of host galaxies.

The *HST* images of 3C 48 reveal tidal tails extending for ~ 35 kpc, which confirms previous suggestions of a strong gravitational interaction in this system. Evidence for a massive host was presented earlier from ground-based imaging and spectroscopy (Boroson & Oke 1982; Malkan 1984; Stockton & Ridgway 1991), observations of CO (Scoville et al. 1993), and far-infrared emission (Neugebauer et al. 1985). The host galaxy of 3C 48 has $M_V = -22.7$ mag, brighter than a typical brightest cluster galaxy ($M_V \approx -22.0$; Hoessel & Schneider 1985 and Postman & Lauer 1995) for $\Omega_0 = 1.0$ and $H_0 = 100$ km s^{-1} Mpc^{-1} and brighter than any host in the 20 member local sample.

The hosts of B2 1425+267 and 3C 345 both have light distributions similar to luminous elliptical galaxies. However, for B2 1425+267, the presence of clumps and a faint galaxy lying within the host galaxy may indicate ongoing gravitational interaction.

All nine RLQs we have studied (either in the local sample or in this paper) observed with *HST* have light distributions consistent with their hosts being elliptical galaxies, or occurring in interacting systems; in some cases there is evidence for both.

9.2. *Hosts of RLQs Are Brighter than Hosts of RQQs*

Several groups have reported on a positive correlation between the luminosity of the active nucleus and that of the host galaxy (McLeod & Rieke 1994b, 1995a; Hooper et al. 1997; Kotilainen, Falomo, & Scarpa 1998). McLeod & Rieke (1995a) and McLeod (1996) suggested that for low-redshift quasars brighter than $M_B \lesssim -22.4$, there is a minimum mass for the host galaxy that increases with increasing nuclear power, implying that a more luminous host galaxy is required to fuel a more luminous quasar. Laor (1998) found a correlation between the luminosity of the quasar host galaxies in the local sample and the inferred (from Hβ) black hole mass. Laor points out that the correlation is similar to the black hole mass versus bulge luminosity correlation found for normal galaxies (Magorrian et al. 1998), which suggests that quasars reside in normal galaxies.

Figure 5 shows the two-dimensional model absolute V magnitudes (from Table 4) of the host galaxies versus the absolute V magnitudes of the quasars (Table 1) in the
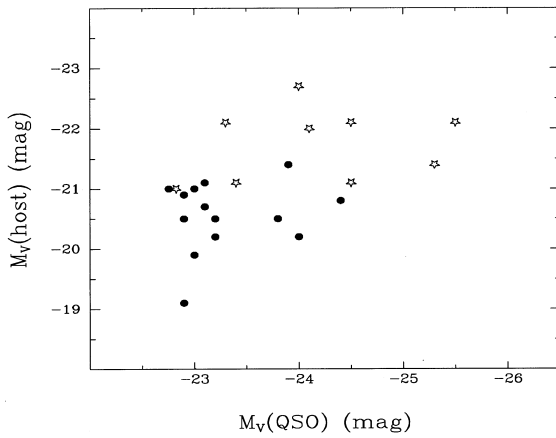
FIG. 5.—Absolute V magnitude of the host galaxies vs. the absolute V magnitude of the quasars. The plotted values include the 20 local sample quasars and the three radio-loud quasars discussed in this paper. The radio-quiet quasars are represented by filled circles, while stars represent the radio-loud quasars.

present study and in the local sample. The best linear fit to all the data yields

$$M_V(\text{host}) = 0.52 \, M_V(\text{QSO}) - 8.67 . \qquad (3)$$

The linear correlation coefficient (Pearson's r) indicates only a 1.3% probability for the optical absolute magnitudes of the quasar and the host to be uncorrelated.

The two most striking aspects of the Figure 5 visible to eye are (1) that there is essentially no correlation of $M_V(\text{host})$ and $M_V(\text{QSO})$ if we consider the RQQs and RQLs separately (probability of no correlation higher than $\sim 50\%$), and (2) the RLQs have host galaxies that are about a magnitude brighter than the host galaxies of RQQs.

Several previous studies have compared the luminosities of the host galaxies of RQQs and RLQs, but a consensus has not been achieved. There are suggestions that the hosts of RLQs are more luminous than the hosts of RQQs (Hutchings et al. 1989; Véron-Cetty & Woltjer 1990; McLeod & Rieke 1995a; Bahcall et al. 1997) and also that there is no significant difference between the host luminosities (Dunlop et al. 1993; Orndahl et al. 1996; Taylor et al. 1996; Hooper et al. 1997).

For the 23 members of our *HST* sample (20 in the local sample and the three RLQs discussed in this paper), the hosts of the RLQs are on average 1 mag brighter than the hosts of the RQQs. The average best-fit two-dimensional model magnitudes for the hosts of the 14 RQQs and nine RLQs are

$$\langle M_V \rangle_{\text{host,RQQ}} = -20.6 \pm 0.2 \text{ mag} , \qquad (4)$$

$$\langle M_V \rangle_{\text{host,RLQ}} = -21.7 \pm 0.2 \text{ mag} , \qquad (5)$$

where the error given is the error of the mean (the standard deviation is $N^{1/2}$ times larger).

We applied the Student's t-test to measure the significance of the difference of means. The probability that the host galaxies of the RLQs and RQQs have the same mean absolute V magnitude is 1.3×10^{-4}. The Kolmogorov-Smirnov test gives a probability of 9×10^{-4} for the distributions of the absolute magnitudes of the host galaxies of the radio-loud and radio-quiet quasars to be the same.

One must view these statistical tests with caution, however, as a glance at Figure 5 shows that the distributions of the optical luminosities of the RQQs and RLQs are significantly different. The four most optically luminous quasars in the entire sample are RLQs, and the average luminosity of the classes differs by nearly a magnitude

$$\langle M_V \rangle_{\text{RQQ}} = -23.3 \pm 0.1 \text{ mag} \quad (14 \text{ objects}) , \qquad (6)$$

$$\langle M_V \rangle_{\text{RLQ}} = -24.2 \pm 0.3 \text{ mag} \quad (9 \text{ objects}) . \qquad (7)$$

If the luminosity of the host depended on the optical luminosity of the quasar, our sample would indicate a RQQ/RLQ difference even if the host galaxy luminosity was independent of quasar radio properties.

We selected a subsample of quasars in which the RLQs and the RQQs have the same absolute magnitude range in order to limit the comparison to quasars with similar optical properties. In the range $-24.5 \le M_V(\text{QSO}) \le -23.2$, there are six RQQs and seven RLQs; both subsamples of quasars have the same average absolute V magnitudes $[\langle M_V(\text{QSO}) \rangle = -23.8$ mag]. For those two subsamples the average best-fit two-dimensional model magnitudes of the host galaxies (and error of the mean) are

$$\langle M_V \rangle_{\text{host,RQQ}} = -20.6 \pm 0.2 \text{ mag} , \qquad (8)$$

$$\langle M_V \rangle_{\text{host,RLQ}} = -21.7 \pm 0.3 \text{ mag} . \qquad (9)$$

The host galaxies of RLQs in this group are on average 1.1 mag (3.1 σ) brighter than the hosts of the RQQs, similar to the result obtained for the whole sample.

Could the difference be an artifact of the galaxy model used in the fitting? This is a concern because of the extrapolations required to calculate the total luminosity; the very center of the galaxy is masked by the quasar, and one can (at best) fit out only to a few effective radii or scale lengths. Since we are restricted to data at intermediate radii, a de Vaucouleurs model fit produces a total magnitude that is systematically brighter than the value obtained with an exponential disk, because the de Vaucouleurs model rises more steeply in the very center and falls more slowly at large radii than does a disk model. For the 23 quasars in our sample, the two-dimensional GdV model gives magnitudes for the host that are on average 0.6 mag brighter than the exponential disk estimates.

For the limited 13 member sample with $-24.5 \le M_V(\text{QSO}) \le -23.2$, we fitted all the hosts with a two-dimensional GdV galaxy model and also with an exponential disk model. In both cases, the hosts of the RLQs are on average 0.8 mag brighter than the hosts of the RQQs (a difference higher than 3 σ), which implies that the difference in the host luminosities of RLQs and RQQs is real.

Figure 6 shows the radio luminosity of the quasars at 6 cm from the Véron-Cetty & Véron (1996) catalog versus the two-dimensional model absolute visual magnitudes of the host galaxies. Figure 6 includes nine RLQs and eight RQQs for which Véron-Cetty & Véron (1996) list a detected emission at 6 cm. This figure shows that the strongest radio sources tend to occur in more luminous host galaxies. As seen in Figure 5, there is no trend for correlation inside the two radio classes. The trend shown in Figure 6 can be represented by a linear regression:

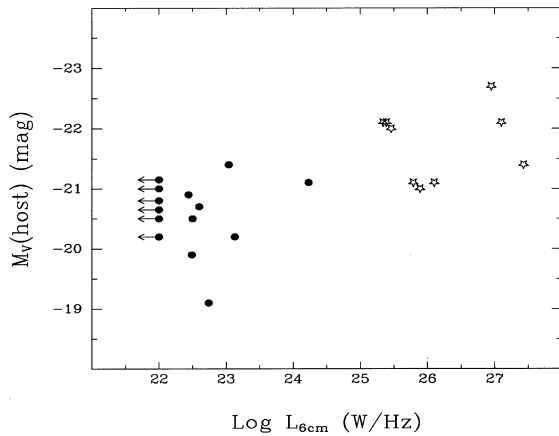$$M_V(\text{host}) = -0.36 \, \log L_{6\,\text{cm}} - 12.33 . \qquad (10)$$

FIG. 6.—Absolute V magnitude of the host galaxies vs. the radio luminosity of the quasars at 6 cm. The flux densities at 6 cm were taken from Véron-Cetty & Véron (1996). Quasars not detected in the radio are indicated by an arrow. The sample and symbols are the same as in Fig. 5.

The linear correlation coefficient indicates that there is less than a 0.1% probability of the luminosity of the host and the quasar radio power being uncorrelated.

We conclude that the difference in the luminosities of the host galaxies of the RLQs and RQQs is significant and robust. The apparent correlation between the optical luminosities of the host and the quasar (Fig. 5) is mainly due to the RLQs occurring in brighter galaxies than the RQQs.

The results suggest that the radio emission of the quasars is connected with the magnitude/mass of the host galaxy, which indicates that only galaxies brighter than a certain limit would be able to harbor a radio-loud quasar.

REFERENCES

Akujor, C. E., Ludke, E., Browne, I. W. A., Leahy, J. P., Garrington, S. T., Jackson, N., & Thomasson, P. 1994, A&AS, 105 247
Angel, J. R. P., & Stockman, H. S. 1980, ARA&A, 18, 321
Bahcall, J. N., Kirhakos, S., Saxe, D. H., & Schneider, D. P. 1997, ApJ, 479, 642
Bahcall, J. N., Kirhakos, S., & Schneider, D. P. 1994, ApJ, 435, L11
———. 1995a, ApJ, 447, L1 (erratum ApJ, 454, L175)
———. 1995b, ApJ, 450, 486
———. 1996a, ApJ, 457, 557
———. 1996b, in Quasar Hosts, ed. D. Clements & I. Perez-Fournon (Berlin: Springer), 37
Balick, B., & Heckman, T. M. 1982, ARA&A, 20, 431
———. 1983, ApJ, 265, 1
Biretta, J. A., et al. 1996, WFPC2 Instrument Handbook, Version 4.0 (Baltimore: STScI)
Block, D. L., & Stockton, A. 1991, AJ, 102, 1928
Boroson, T. A., & Oke, J. B. 1982, Nature, 296, 397
———. 1984, ApJ, 281, 535
Boroson, T. A., Oke, J. B., & Green, R. F. 1982, ApJ, 263, 32
Boroson, T. A., Person, S. E., & Oke, J. B. 1985, ApJ, 293, 120
Boyce, P. J., et al. 1996, ApJ, 473, 760
Canalizo, G., Stockton, A., & Roth, K. C. 1998 AJ, 115, 890
de Vaucouleurs, G. 1948, Ann. d'Ap., 11, 247
Disney, M. J., et al. 1995, Nature, 376, 150
Dunlop, J. S., Taylor, G. L., Hughes, D. H., & Robson, E. I. 1993, MNRAS, 264, 455
Ellingson, E., & Yee, H. K. C. 1994, ApJS, 92, 33
Fanti, C., Fanti, R., Dallacasa, D., Schillizzi, R. T., Spencer, R. E., & Stanghellini, C. 1995, A&A, 302, 317
Fisher, K. B., Bahcall, J. N., Kirhakos, S., & Schneider, D. P. 1996, ApJ, 468, 469
Fukugita, M., Shimasaku, K., & Ichikawa, T. 1995, PASP, 107, 945
Goldsmith, D. W., & Kinman, T. D. 1965, ApJ, 142, 1693
Hoessel, J. G., & Schneider, D. P. 1985, AJ, 90, 1648
Hooper, E., Impey, C. D., & Foltz, C. B. 1997, ApJ, 480, 95
Hutchings, J. B., & Campbell, B. 1983, Nature, 303 584
Hutchings, J. B., Crampton, D., & Campbell, B. 1984, ApJ, 280, 41
Hutchings, J. B., Holtzman, J., Sparks, W. B., Morris, S. C., Hanisch, R. J., & Mo, J. 1994, ApJ, 429, L1
Hutchings, J. B., Janson, T., & Neff, S. G. 1989, ApJ, 342, 660
Hutchings, J. B., & Morris, S. 1995, AJ, 109, 1541
Hutchings, J. B., & Neff, S. G. 1992, AJ, 104, 1
Kollgaard, R. I., Wardle, J. F. C., & Roberts, D. H. 1989, AJ, 97, 1550

Kotilainen, J. K., Falomo, R., & Scarpa, R. 1998, A&A, 332, 503
Krist, J. 1993, in ASP Conf. Ser. 52, Astronomical Data Analysis Software and Systems II, ed. R. J. Hanish, R. J. V. Brissenden, & J. Barnes (San Francisco: ASP), 530
Kristian, J. 1973, ApJ, 179, L61
Kukula, M. J., Dunlop, J. S., Hughes, D. H., Taylor, G., & Boroson, T. 1996, in Quasar Hosts, ed. D. Clements & I. Perez-Fournon (Berlin: Springer), 177
Laor, A. 1998, ApJ, 505, L83
Magorrian, J., et al., 1998 AJ, 115, 2285
Malkan, M. A. 1984, ApJ, 287, 555
Matthews, T. A., Bolton, J. G., Greenstein, J. L., Munch, G., & Sandage, A. R. 1961, Sky and Telesc., 21, 148
McLeod, K. K. 1996 in Quasar Hosts, ed. D. Clements & I. Perez-Fournon (Berlin: Springer), 45
McLeod, K. K., & Rieke, G. H. 1994a, ApJ, 420, 58
———. 1994b, ApJ, 431, 137
———. 1995a, ApJ, 441, 96
———. 1995b, ApJ, 454, 80
Neugebauer, G., Soifer, B. T., & Miley, G. K. 1985, ApJ, 295, L27
Orndhal, E., Ronnback, J., & van Groningen, E. 1996, in Quasar Hosts, ed. D. Clements & I. Perez-Fournon (Berlin: Springer), 217
Postman, M., & Lauer, T. R. 1995, ApJ, 440, 28
Rogola, A., Padrielli, L., & de Ruiter, H. R. 1986, A&AS, 64, 557
Schraml, J. Pauliny-Toth, I. I. K., Witzel, A., Kellerman, K. I., Johnston, K. J., & Spencer, J. H. 1981, ApJ, 251, L57
Scoville, N. Z., Padin, S., Sanders, D. B., Soifer, B. T., & Yun, M. S. 1993, ApJ, 415, L75
Simon, R. S., Readhead, A. C. S., Moffat, A. T., Wilkinson, P. N., Booth, R., Allen, B., & Burke, B. F. 1990, ApJ, 354, 140
Stockton, A., & MacKenty, J. W. 1983, Nature, 305, 678
———. 1987, ApJ, 316, 584
Stockton, A., & Ridgway, S. E. 1991, AJ, 102, 488
Taylor, G. L., Dunlop, J. S., Hughes, D. H., & Robson, E. I. 1996, MNRAS, 283, 930
Véron-Cetty, M. P., & Véron, P. 1996, A Catalogue of Quasars and Active Nuclei (ESO Sci. Rep. 17) (7th ed.; ESO: Garching)
Véron-Cetty, M. P. & Woltjer, J. 1990, A&A, 236, 69,
Wampler, E. J., Robinson, L. B., Burbidge, E. M., & Baldwin, J. A. 1975, ApJ, 198, 49
Wyckoff, S., Gehren, T., Morton, D. C., Albrecht, R., Wehinger, P. A., & Boksenberg, A. 1980, ApJ, 242, 59